Key features of the innate immune response is mediated by the immunoproteasome in microglia

Salman Izadjoo
Uniformed Services University
Kasey E. Moritz
Uniformed Services University
Guzal Khayrullina
Uniformed Services University
Elizabeth M. Bergman
Uniformed Services University
Brendan M. Melvin
Uniformed Services University
Matthew W. Stinson
Uniformed Services University
Summer G. Paulson
Uniformed Services University
Nikki M. McCormack
Uniformed Services University
Kelsey N. Anderson
University of Maryland
Lunndon A. Lewis
Uniformed Services University
Jeremy D. Rotty
Uniformed Services University
Barrington G. Burnett
barrington.burnett@usuhs.edu
Uniformed Services University

Article

Keywords: Immunoproteasome, Microglia, Innate immunity, Complement, Cytokines, NFκ-B, Phagocytosis, ONX-0914

Posted Date: June 6th, 2024

DOI: https://doi.org/10.21203/rs.3.rs-4467983/v1

Additional Declarations: No competing interests reported.

Abstract

Microglia are the resident immune cells of the central nervous system (CNS). We and others have shown that the inflammatory response of microglia is partially regulated by the immunoproteasome, an inducible form of the proteasome responsible for the generation of major histocompatibility complex (MHC) class I epitopes. While the role of the proteasome in the adaptive immune system is well established, emerging evidence suggests the immunoproteasome may have discrete functions in the innate immune response. Here, we show that inhibiting the immunoproteasome reduces the IFNγ-dependent induction of complement activator C1q, suppresses phagocytosis, and alters the cytokine expression profile in a microglial cell line and microglia derived from human inducible pluripotent stem cells. Moreover, we show that the immunoproteasome regulates the degradation of IκBα, a modulator of NF-κB signaling. Finally, we demonstrate that NADH prevents induction of the immunoproteasome, representing a potential pathway to suppress immunoproteasome-dependent immune responses.

Main Points

- The immunoproteasome regulates complement gene expression and chemokine production in microglia.
- Inhibiting the immunoproteasome reduces microglia phagocytic activity.
- Inhibiting the immunoproteasome decrease IFNγ-dependent IκBα degradation in microglia.
- NADH suppresses immunoproteasome induction.

INTRODUCTION

As immune cells of the central nervous system (CNS), microglia constantly survey the brain and spinal cord for changes to the local environment. In response to CNS infection or injury, microglia transition to a reactive state, where they are responsible for mounting an immune response. The adaptive immune response occurs over a period of days to weeks and is more specific to particular pathogens or invaders. The innate immune response in the CNS is primarily mediated by microglia and is activated within hours of pathogen recognition (For review, [1]). There are three major components of the innate immune response. First, activation of the complement cascade activates additional immune cells, facilitating identification of bacteria, dying cells and foreign pathogens. The complement system can also target invading cells for destruction. Second, dead cells, foreign particles and cell debris are cleared by phagocytosis. Finally, the innate immune response involves production of cytokines and chemokines which act to promote cell migration and recruitment of additional immune cells to the site of injury or infection.

Activation of microglia and the subsequent innate immune response is critical for defense against infection, however, during trauma, it can have confounding effects. The inflammatory response is important for returning the CNS to homeostasis, however increased microglia reactivity and the subsequent inflammatory response can result in reduced functional recovery following trauma and

stroke. In addition, persistent activation of the immune response can result in an exacerbated response to subsequent injuries. Decreasing inflammation following trauma can reduce some of the long-term functional deficits associated with CNS injury. Furthermore, neuroinflammation has been linked to neurodegenerative disease progression such as in Alzheimer's and Parkinson's diseases [2,3]. Thus, controlling the inflammatory response of microglia following CNS disruption could prove to be a beneficial therapeutic option.

Protein degradation machinery lies at the intersection of cellular homeostasis and neuroinflammation. The proteasome is the final destination for proteins tagged for degradation by the ubiquitin proteasome system [4]. During trauma, infection and subsequent neuroinflammation, the constitutive proteasome subunits are replaced by immunoproteasome subunits [5,6]. The inducible immunoproteasome has alternative regulator and catalytic subunits than the constitutive proteasome (For review, [7]). IFNγ, a pro-inflammatory cytokine up-regulated during CNS trauma triggers the formation of the immunoproteasome. We have previously reported that inhibiting the immunoproteasome alters the microglia transcriptome profile, most notably in regards to the immune response and inflammation [6]. While the immunoproteasome has been shown to be critical in peptide processing for antigen presentation during the adaptive immune response, there have been few studies to date that link the immunoproteasome and the innate immune response in microglia [7]. We thus sought to examine the role of the immunoproteasome on the innate immune response of microglia and investigate the mechanism of immunoproteasome mediation of inflammation. Our study demonstrates that pharmacological and genetic ablation of the immunoproteasome subunit β5i reduces IFNγ-dependent expression of the classical complement system activator C1q, phagocytosis, and chemokine production. In addition, we demonstrate that genetic ablation of β5i results in reduced IκBα degradation, signifying increased NF-κB activation, providing insight into a possible mechanism of immunoproteasome-mediated inflammatory response in microglia. Finally, we show that NADH, a known inhibitor of microglia-mediated neuroinflammation, blocks IFNγ-mediated induction of the immunoproteasome. Taken together, this study provides initial evidence that the immunoproteasome mediates key features of the innate immune response in mouse and human microglia exposed to IFNγ.

MATERIALS AND METHODS

Cell Culture

BV-2 cells were cultured under standard conditions in DMEM (Thermofisher) medium containing 5% FBS (Sigma), 2 mM L-Glutamine, 100 units/ml penicillin and 100 µg/ml streptomycin (Thermofisher). Cells were passaged 2-3 times per week. CRISPR/Cas9-mediated β5i knock-out BV-2 cells were created as previously described [6]. We obtained doxycycline inducible microglia IPSCs from Dr. Michael Ward's lab [8]. Ward [9]. IPSC lines were maintained in standard 6-well tissue culture plates coated with growth factor reduced Matrigel (Cat. 354277, Corning) or Geltrex (Cat. A1569601, Gibco) diluted 1:100 in DMEM/F12 (Gibco) on the same day as iPSC plating. Frozen stocks of iPSCs were thawed and plated on Matrigel or

Geltrex coated plates in Essential 8™ Basal Medium (Gibco) supplemented with 10μM ROCK inhibitor (Y-27632 dihydrochloride; Tocris #1254). iPSC lines were passaged using 0.5 mM EDTA in PBS without $CaCl_2$ and $MgCl_2$ (Life Technologies). Cells were maintained in incubators at 37°C, 5% CO_2. The iPSCs and differentiated cells were confirmed to be mycoplasma negative.

IPSC Microglia Differentiation

Doxycycline-inducible microglia iPSCs were grown in StemFlex or Essential 8™ Basal Medium (Gibco) until reaching at least 50% confluency and were grown for at least 24 h without ROCK inhibitor (Tocris #1254). Cells were dissociated, centrifuged and pelleted cells were resuspended in Day 0 differentiation medium containing the following: Essential 8™ Basal Medium as a base, 10μM ROCK inhibitor, and 2 μg/ml Doxycycline (Clontech). Doxycycline inducible microglia iPSCs were counted and seeded onto double coated plates (Poly-D-Lysine-precoated Bio plates (Corning) + Matrigel or Geltrex coating) with 350,000 cells per /well for a 6-well plate. Media was replaced on day 2 with differentiation media consisting of Advanced DMEM/F12 Medium (Gibco) as a base medium , 100X GlutaMAX™ (Gibco), 2 μg/ml doxycycline, 100 ng/ml Human IL34 (Peprotech) and 10 ng/ml Human GM-CSF (Peprotech). On day 4, the medium was replaced with maintenance Microglia medium, containing Advanced DMEM/F12 as a base medium combined with 100X Antibiotic-Antimycotic (1X Anti-Anti) (Gibco), 100X GlutaMAX, 2 μg/ml doxycycline, 100 ng/ml Human IL-34 and 10 ng/ml Human GM-CSF, 50 ng/ml Human M-CSF (Peprotech) and 50 ng/ml Human TGFB1 (Peprotech), and 50 uM Mevalonate (Sigma). On Day 8, half the media was replaced with fresh Microglia medium. Microglia were cultured for up to 12 additional days in maintenance Microglia medium with full medium changes every 3-4 days. Cells were assayed on day 9.

Cytokine and Drug Treatment

BV-2 cells were plated 60-70% confluent, allowed to adhere overnight then treated with 200 U/mL of IFNγ (R&D Systems) for 24 h. Immunoproteasome inhibition was achieved using 100 nM ONX-0914 (UBPBio). Cells requiring nicotinamide adenine dinucleotide treatment were pre-treated for 24 h (100 μM, Sigma-Aldrich).

RNA Isolation and Gene Expression Analysis

Gene expression analysis was performed as previously described [6]. Briefly, RNA was isolated by the Trizol and chloroform extraction method, then purified RNA was then converted to cDNA using a Veriti thermal cycler and a high capacity cDNA conversion kit (Applied Biosystems). Gene levels were measured using pre-validated Taqman probes (Life Technologies).

Western and Native Gel Electrophoresis

For western blotting, cells were lysed (20 mM Hepes, .32 M Sucrose, 5 mM $MgCl_2$, 2 mM ATP, .2% W/V NP-40, 2 mM DTT, Protease Inhibitor, pH 7.2), combined with sample buffer on run on 4-12% gels

(Invitrogen). All antibodies were obtained from Abcam unless otherwise stated: Psmb5 (ab3330), Psmb8 (ab3329), IκBα (sc371, Santa Cruz), β actin (A3854, Sigma), C1q (ab71089), IP-10 (MAB466, R&D Systems), CCL2 (NBP1-07035, Novus Biologicals).

Flow Cytometry

Cells were prepared for flow cytometry as previously described [6]. Briefly, cells were rinsed with warm PBS, then dislodged by scraping in FACS buffer (ThermoFisher). Following, cells were spun down at 1400 RPM at room temperature for 5 min. Samples were then incubated with pre-conjugated antibodies from Biolegend (anti-CR1/2, anti-CR3, anti-CD88, and anti-CD93).

Phagocytosis Assay

BL-21 DE3* (ThermoFisher) were transformed with pAcGFP1 vector as described previously [10]. 40 µl of bacteria (3.0×10^8) were combined with 1 ml of culture media and added to each well of BV-2 cells which had been pre-treated with 200 U/mL IFN γ and/or 100nM ONX-0914 for 24 h. Cells were incubated at 37 °C for 30 min then washed 3 times with ice-cold PBS before being dislodged by scraping with FACS buffer and submitted to flow cytometry (BD Accuri C6, BD Biosciences). Cells were gated so that only viable cells were counted. 10,000 cells per treatment group were counted. To adjust for background, control cells that were not incubated with E. coli were used for each experiment (n=6). The percentage of GFP positive cells was measured and data were analyzed using an ANOVA with Tukey's *post hoc* analysis.

Real-time phagocytosis functionality was assessed using a bead-based assay. IgG (Sigma-Aldrich, 12-371) was first labeled with pHrodo™ iFL Red following the manufacturer's instructions (ThermoFisher Scientific, Cat# P36014). Subsequently, 60 µg of labeled IgG was opsonized with 60 µL of 2 µm Polybead Carboxylate Microspheres (Polysciences, Inc, 18327-10) in 500 µL of 1X PBS. The IgG-opsonized beads were then vigorously vortexed. Cells were seeded into a 24-well plate at a desired density. Following cell attachment, 4 µL of the opsonized beads were added to each well and the plate was gently shaken to ensure even distribution. The phagocytosis assay was then run on a Cytation 5 Imaging Reader. Images were captured every 15 minutes for 2 hours using both Relief Contrast and TRITC channels. Four positions within each well were imaged. After the 2-hour incubation, the media was aspirated from the wells. Cells were then stained with a 1:10,000 dilution of Hoechst stain in 1X PBS for 5 minutes. Following thorough washing with PBS, a final image was captured using Relief Contrast, TRITC, and DAPI channels.

Quantification was performed using the Cytation 5 software. The software was used to count the number of cells in the DAPI channel and to measure the number, size, and intensity of phagosomes in the TRITC channel. Data analysis was then performed using the software outputs. The ratio of phagosomes to cell number, the difference in phagosome intensity per condition, and the difference in phagosome average area per condition were all calculated.

Cytokine Panel

The Proteome Profiler Mouse Cytokine Array Panel Cytokine expression was used to measure cytokine expression at 24 hours post-treatment (R& D systems, Minneapolis, MN). The assay was conducted per the manufacturer's instructions. 300µg of protein was collected from cell lysates (n=4 per group). HLImage++ machine vision and image processing software with Array QuickSpots was used to analyze the cytokine expression density (2011 Western Vision Software). Duplicate spots representing individual cytokines were averaged and background was subtracted. For statistical analysis, all spots that were not detectable were counted as 0. Data are normalized to the IFNγ treatment group.

Data Analysis

All data were analyzed using SPSS24 or Graphpad Prism for Windows. Outliers were removed by calculating the Z-score (95% confidence interval) for each data set. Data points where Z>2 were considered outliers and omitted from analysis. For analysis between 2 groups (Control and IFNγ, sham and injury, BV-2 WT and BV-2 β5i KO) an independent samples t-test (2-tailed) was conducted. Levene's test was used to assess variance and normality and appropriate transformations were applied when necessary. For experiments involving multiple treatment groups, one-way analysis of variance was used (ANOVA), with Tukey's HSD *post-hoc* to compare differences between groups when appropriate. For all figures, *p<.05, **p<.01, ***p <.001, ****p<.0001. Data are presented as mean values ± standard error of the mean (SEM).

RESULTS

Immunoproteasome inhibition decreases IFNγ-dependent activation of the complement cascade.

Reactive microglia have increased activation of the complement cascade, which can promote neural necrosis and inflammation [11]. BV-2 cells are an immortalized microglia cell line that, upon induction by IFNγ, express immunoproteasomes at approximately the same level as primary microglia [5,6]. In addition, BV-2 cells express complement genes similar to primary brain and retinal microglia [12]. Activation of the classical complement cascade begins when C1q, a fluid phase complement activator, binds to apoptotic cells or other microbes and debris, [13]. Given that C1q promotes microglial reactivity, we sought to examine the role of the immunoproteasome on complement activation. We treated BV-2 cells with IFNγ and measured the C1q gene cluster, C1qa, C1qb and C1qc expression via qRT-PCR. We found that IFNγ treatment resulted in significantly higher gene expression of all 3 genes (p<.001, p<.001, and p<.001, respectively), which was abrogated in the presence of an immunoproteasome inhibitor (Figure 1A-C). To confirm that loss of immunoproteasome activity suppressed complement gene activation we utilized BV2 cells where the catalytic β5i subunit was deleted (BV-2 β5i KO). Interestingly, we found low basal expression of each C1q gene in BV-2 β5i KO cells (Figure 1A-C). Moreover, IFNγ-dependent complement gene induction is blocked in BV-2 β5i KO cells (Figure 1A-C), consistent with pharmacological inhibition of immunoproteasome activity. In addition to gene expression, C1q protein

levels were upregulated by IFNγ in WT BV-2 cells. This IFNγ-dependent increase in C1q protein levels was reduced in β5i KO BV-2 cells compared to WT BV-2 cells (Figure 1D).

C3 is a major component of the complement immune system, involved in both the classical and lectin complement pathways and is important for tagging pathogens, extracellular protein plaques such as amyloid beta, and other foreign complexes for phagocytosis [14,15]. C3 is synthesized under basal conditions but can be stimulated by IFNγ [16]. We measured C3 gene expression in the absence or presence of IFNγ and immunoproteasome inhibitor ONX-0914. We found that ONX-0914 treatment reduced basal levels of C3 expression compared to control (Figure 1E). Further, IFNγ and ONX-0914 co-treatment reduced C3 expression compared to IFNγ alone (Figure 1E). These data suggest that the immunoproteasome regulates C3 expression.

C3b tagged pathogens or complexes are recognized by microglia via the C3b receptor, Cr1 (also known as CD35) [17,18]. It has been previously reported that IFNγ decreases Cr1 levels on human monocytes in a dose dependent manner [19]. Given that immunoproteasome inhibition reduced the IFNγ-dependent increase in C1q, we sought to determine if IFNγ and/or the immunoproteasomes alter complement receptors in BV-2 microglia. We found the levels of the complement receptors Cr1/2 or Cr3 levels were unchanged following IFNγ, ONX-0914 or co-treatment (Supplemental Figure 2A-B). Interestingly, C1q receptor (CD93) levels were reduced in the presence of IFNγ, but was not reduced by ONX-0914 co-treatment (Supplemental Figure 2C). The levels of the complement receptor C5aR (CD88) were also unchanged between groups (Supplemental Fig. 2D). Together, these data suggest that the immunoproteasome plays a critical role in complement activation by modulating C1q induction independent of complement receptor expression.

Given the growing evidence demonstrating differences in human and mouse microglia, we next sought to confirm that the immunoproteasome regulated IFNγ-dependent complement gene induction in human microglia cells. We utilized a doxycycline inducible human inducible pluripotent stem cells (iPSCs) microglia line that expresses crucial microglia markers and adopts a ramified morphology 8 days after differentiation. We then wanted to confirm that our iPSC-derived microglia expressed immunoproteasome subunits in the presence of IFNγ. We found all immunoproteasome catalytic subunits exhibited increased gene expression after exposure to IFNγ (Supplemental Figure 1A-C). We treated iPSC-derived microglia with IFNγ and measured C1qa, C1qb and C1qc expression by qRT-PCR. Consistent with findings in mouse microglia, IFNγ treatment resulted in robust induction of C1q gene cluster, which was reversed in the presence of the immunoproteasome inhibitor (Fig. 1F). Together, our findings suggest that the immunoproteasome regulates IFNγ-dependent complement activation in mouse and human microglia.

Phagocytosis is slowed by immunoproteasome inhibition

Phagocytosis is a major component of innate immunity, and we have previously shown that immunoproteasome inhibition decreased phagocytosis of carboxylate-modified microspheres [6]. IgG-

mediated phagocytosis is one mechanism employed by microglia to recognize and engulf pathogens [20]. To test whether immunoproteasomes were involved in IgG-mediated phagocytosis, we treated BV-2 cells with ONX-0914 for 24h ours, then incubated cells with FITC-conjugated, IgG-coated latex beads. We found that ONX-0914 treatment reduced microglial-mediated phagocytosis of IgG-coated beads (Figure 2A). This finding was reproduced in β5i KO BV-2 cells, demonstrating that the effect on phagocytosis was not due to off -target effects of ONX-0914. We next tested if phagocytosis of E. coli, a more physiological relevant substrate, was impaired by inhibition of the immunoproteasome. We incubated cells with GFP-expressing E. coli for 30 m, in the presence or absence of ONX-0914, then subject the cells to flow cytometry to measure the percentage of cells that were GFP^+ [10]. BV-2 cells treated with ONX-0914 did not engulf E. coli as effectively as control cells, resulting in reduced percentage of GFP^+ cells compared to control (Figure 2B). Similar to the effect seen in phagocytosis of IgG-coated beads, the phagocytosis of E.coli was significantly reduced in the β5i KO BV-2 cells.

Additionally, WT and β5i KO BV-2 cells plated in glass chambers and treated with 2-micron beads coated with pHrodo-opsonized IgG showed a significant difference in phagocytosis at the end of 2 hours. The β5i KO BV-2s demonstrated a decrease in phagocytosis of these IgG coated beads, as seen through visualizing the red fluorescence of the internalized pHrodo label in cells when compared to WT BV-2s (Figure 2C). When comparing the fluorescence across cell types, WT BV-2s generate more phagosomes with higher fluorescence intensity than β5i KO BV-2s (Figure 2D). Taken together, these data indicate that the immunoproteasome has a global effect on phagocytosis, regardless of the substrate being engulfed, suggesting that it controls a cellular mechanism common to the different types of phagocytosis.

IFNγ-dependent cytokines are modulated by immunoproteasome inhibition

In addition to complement activation and phagocytosis, cytokine release is a major feature of the innate immune response. During infection, release of cytokines and chemokines initiate the inflammatory response, facilitating debris clearance, immune cells recruitment and subsequent protection from infection. During trauma and ageing, however, blood brain barrier (BBB) dysfunction and recruitment of peripheral immune cells to the CNS are detrimental side-effects of cytokine production and release [21,22]. We next performed an unbiased cytokine protein array to examine the relative amounts of various cytokines produced by BV-2 cells exposed to IFNγ (Figure 3A-B and Table 1). We found that IFNγ significantly increased the levels of 11 cytokines examined, compared to control (p<.05). Furthermore, we found that co-treatment with ONX-0914 significantly reduced the levels of 4 of these cytokines compared to IFNγ treatment alone. Interestingly, not all the cytokines that were up-regulated by IFNγ were reduced by ONX-0914, suggesting that the immunoproteasome mediates a specific sub-set of IFNγ-induced cytokines. These results were consistent in β5i KO BV-2 cells, suggesting that ONX-0914 off-target effects did not affect cytokine secretion (Figure 3C).

Table 1: Mean cytokine levels.

	Control	IFNγ	ONX-0914	IFNγ+ONX-0914
BLC	866.50	1218.27	1508.71	1337.00
C5/C5a*	467.32	811.13	969.00	891.92
G-CSF*	151.79	465.61	534.88	411.57
GM-CSF	Undetected	164.42	275.10	174.34
sICAM-1	14824.16	22037.30	21240.40	21870.84
IL-1ra*	3096.32	10518.27	4585.73	7466.45
IL-2	808.91	373.07	117.85	264.98
IL-3	792.38	1260.42	1407.41	1469.89
IL-4*	416.19	767.21	922.63	825.54
IL-5	84.65	380.33	393.02	290.82
IL-6	Undetected	168.73	209.51	60.62
IL-27*	51.76	387.53	189.89	255.20
IP-10**	1389.76	21515.35	1971.25	14879.69
I-TAC*	429.45	752.20	907.04	800.80
KC	93.74	379.99	384.28	208.07
M-CSF	9.02	401.14	453.96	74.95
MCP-1**	1029.59	2077.57	1458.85	885.17
MIG**	Undetected	3707.30	35.24	1916.18
MIP-1alpha	7084.88	4003.13	9256.91	2516.37
RANTES**	Undetected	932.45	47.91	270.62
SDF-1*	414.34	1229.00	1130.33	866.24
TARC	834.81	1133.93	1417.26	1343.51
TIMP-1	726.10	1129.15	1389.80	1177.04

BV-2 cells were treated for 24 hours then submitted to cytokine analysis. Values are mean pixel density of 4 independent experiments. * indicates a significant difference between control and IFNγ groups. ** ($p<0.05$) indicates that ONX-0914 treatment reversed the IFNγ–dependent increase.

The immunoproteasome mediated cytokines include Cxcl10, MIG, MCP-1, and RANTES. Cxcl10 (also known as IP-10) is a chemokine released by multiple cell types which binds to its receptor; Cxcr3, activating and facilitating microglia migration to sites of injury [23]. Binding of Cxcl10 to neurons has been

linked to neuronal death, highlighting the importance of understanding the mechanisms of modulating Cxcl10 levels [24]. We found that Cxcl10 is increased following IFNγ treatment, however when cells are co-treated with ONX-0914, this effect is diminished (Figure 3A-B). Another ligand that binds to Cxcr3, resulting in microglia activation and immune cell recruitment, is MIG (also known as Cxcl9) [25]. Here we found that MIG levels are increased following IFNγ treatment, which is abrogated in the presence of ONX-0914.

Monocyte Chemotactic and Activating Factor, MCP-1, (also known as Ccl2) is released by microglia during trauma and infection, and is also a key modulator of neuropathic pain [26]. Microglia lacking MCP-1 are less activated and have reduced motility, resulting in improved histological and behavioral outcomes following intracerebral hemorrhage in mice [27]. We found that IFNγ increased MCP-1 in BV-2 microglia, an effect that was blocked when cells were co-treated with the immunoproteasome inhibitor (Figure 3A-B).

RANTES (also known as Ccl5) is a chemokine that is up-regulated in response to trauma and other neurological diseases that, in addition to its chemo attractant properties, induces microglia to a pro-inflammatory state [28]. Inhibition of RANTES reduces neuroinflammation and decreases BBB permeability, thus decreasing RANTES levels during chronic inflammation could prove useful [29]. Here we show that IFNγ significantly increases RANTES protein levels, but not when cells were co-treated with ONX-0914 (Figure 3A-B). In addition, we showed that the IFNγ-dependent induction of each chemokine was blocked in BV-2 cells where the β5iβ subunit was knocked out, confirming the findings observed with ONX-0914 treatment (Figure 3C).

Given human and mouse chemokines may be differentially regulated, we next sought to determine if the chemokines we identified in mouse BV-2 cells were similarly immunoproteasome-dependent in human microglia. Inducible human iPSC-derived microglia were exposed to IFNγ and the expression of the select chemokines were determined by qRT-PCR. We found that Cxcl10, MCP-1, and RANTES expression were increased in the presence of IFNγ (Supplemental Figure 3CB). This IFNγ-dependent induction of each chemokine was suppressed when cells were co-treated with ONX-0914. We did not detect the presence of MIG in iPSC-derived microglia. Taken together, we show that the immunoproteasome mediates multiple chemokines that are primarily related to chemotaxis, responsible for microglial motility, and immune cell recruitment.

Altered microglia innate immune response is due to immunoproteasome regulation of NF-κB

In addition to complement activation and phagocytosis, MIG [30], RANTES [31], MCP-1 [32] and Ip-10 [33] have all been shown to be transcriptionally regulated by NF-κB, so we sought to determine whether loss of the immunoproteasome subunit β5i altered IκBα degradation, a surrogate marker of NFκB activation. We treated WT and β5i KO BV-2 cells with IFNγ over the course 4 hours and analyzed IκBα protein levels. We found that IκBα was significantly reduced after 20 minutes of IFNγ treatment in WT BV-2 cells (Figure 4 A-B). However, later time points resulted in no significant change compared to untreated cells (0 minutes) (Figure 4A-B). This suggests that IFNγ signaling exhibits peak IκBα degradation 20 minutes

post-stimulation and begins resynthesis at 40 minutes post-stimulation. Interestingly, IκBα was stabilized in the β5i KO BV-2 cells as we observed no significant change in IκBα degradation over time compared to control (Figure 4A, B). Concomitantly, IκBα basal levels were significantly greater in β5i KO BV-2 cells compared to WT BV-2 cells prior to IFNγ treatment (Figure 4A, B).

Cox-2 is a well-known downstream gene target of NF-κB which, when NF-κB is inhibited, Cox-2 gene expression is also inhibited. As a measure of NF-κB activity, we measured gene expression levels of Cox2 in the absence and presence of IFNγ and/or ONX-0914 treatment. We found that IFNγ treatment increased Cox2 levels (Figure 4C). The IFNγ-dependent increase in Cox-2 expression was blocked when cells were co-treated with ONX-0914 (Figure 4C). These data are consistent with the reduced IκBα degradation in β5i KO BV-2 cells, providing further evidence that immunoproteasome inhibition decreases IFNγ-dependent NF-κB activation.

NADH reduces immunoproteasome levels and complement gene expression.

Extracellular Nicotinamide Adenine Dinucleotide (NAD) concentrations are basally low, however, it is released in high amounts during inflammation [34]. Exogenous NAD has been previously shown to decrease microglia activation following traumatic brain injury [35]. Interestingly, it has been reported that endogenous NAD^+ can get taken up by cells, converted to NADH, and stabilize the constitutive proteasome [36]. Thus, we looked to determine if NADH treatment modulated the microglia inflammatory response via stabilization of the constitutive proteasome and subsequent suppression of immunoproteasome assembly. Pre-treatment of cells with NADH blocked IFNγ-dependent induction of the β5i subunit (Figure 5A) and assembly of the immunoproteasome (Figure 5B). We found a significant reduction in the expression of the complement protein C1qa, demonstrating a functional consequence of NADH treatment (Figure 5C).These data suggest that assembly of the immunoproteasome can be blocked by stabilizing the constitutive proteasome.

DISCUSSION

The proteasome is responsible for the selective degradation of most intracellular proteins and regulates inflammatory and immune responses. Based on transcriptome analysis from our previous study we hypothesized that the immunoproteasome played a role in both adaptive and innate immune responses. The goal of this study was to examine which aspects of the microglial innate immune response are mediated by the immunoproteasome. We found three central components of the innate immune response, activation of the complement cascade, phagocytosis and cytokine release, were all impacted by immunoproteasome inhibition, consistent with a critical role of the immunoproteasome in the microglial innate immune response.

The immunoproteasome and the innate immune response

Microglia are the dominant source of complement activation protein, C1q, in the brain [37]. Activation of the complement cascade in microglia has implications seen in multiple neurodegenerative diseases. Microglial reactivity, complement activation and pro-inflammatory cytokine release are commonly reported in Alzheimer's Disease (AD) (For review, [38]). However, recent evidence shows microglia may not just respond to injury, but may actually precede and exacerbate neuropathology [39]. One of the neuropathological hallmarks of AD is synaptic loss, which microglia have been shown to facilitate via complement mediated synaptic pruning [40,41]. In neurodegenerative diseases such as AD and Parkinson's disease (PD), as well as after traumatic brain injury (TBI), phagocytosis is critical for clearance of dying cells. Contrary to this, several studies have suggested that phagocytosis may exacerbate neuronal death during inflammation, promoting neurodegeneration [42-46]. Bacterial infection is one of the major activators of the innate immune system and there is some evidence suggesting a role of bacterial infection in the pathogenesis of AD [47]. Thus, tight regulation of phagocytosis during and after inflammation is critical to maintain a healthy balance between debris clearance and unwanted neuronal phagocytosis. In the current study, we demonstrate that genetic ablation of β5i and -treatment with immunoproteasome inhibitors slows phagocytosis through different mechanisms, suggesting that there are potentially multiple converging immunoproteasome-dependent phagocytosis pathways in microglia. Better understanding of this process will allow us to devise mechanisms to maintain the proper balance between clearance of debris and over-activation of phagocytosis.

In addition to phagocytic activity, microglia rapidly release several cytokines and chemokines in response to infection or injury which act to limit the toxic insult and recruit other immune cells. In the current work we found that immunoproteasome inhibition selectively alters levels of some cytokines, but does not have a global effect on all cytokines measured. Cxcl10, RANTES, MIG, and MCP-1 are all chemoattractant molecules that help facilitate cellular migration, recruitment of microglia and peripheral immune cells to the site of damage. Following a CNS lesion, microglia migrate to the site of damage in an IP-10 dependent manner, resulting in dendritic degeneration. IP-10 receptor knockout, spares dendritic degeneration by microglia [23]. Our finding reveals that IFNγ stimulates microglia to release specific chemoattractants through an immunoproteasome-dependent mechanism, potentially influencing neuronal degeneration following an injury.

The immunoproteasome regulates NF-κB

Upon degradation of IκBα, the p65 subunit of NFκB is translocated to the nucleus to activate the transcription of a large amount of immune response-related genes. There have been conflicting reports regarding whether the immunoproteasome more efficiently degrades IκBα compared to the constitutive proteasome [48,49]. Here we report that in response to IFNγ, IκBα is stabilized in β5i KO BV-2 cells, suggesting. This the immunoproteasome regulates IκBα turnover and subsequent IFNγ-dependent NFκB activation.

Stabilizing the constitutive proteasome inhibits aspect of IFNγ-dependent microglial activation

NAD is a coenzyme that is found in all cells and is most commonly studied for its role in metabolism. However, recent studies have implicated decreased NAD levels in aging and neurodegeneration [50]. Another, somewhat less investigated function of the reduced form of NAD, NADH, is its ability to bind and stabilize the constitutive proteasome [36]. We and others have reported that IFNγ results in the loss of constitutive proteasome levels; however, we recently suggested that immunoproteasome subunits are inserted into pre-existing constitutive proteasomes, following disassembly [6,51]. Interestingly, data from this study support our previous findings; as cells pre-treated with NADH, which stabilizes the constitutive proteasome, have reduced levels of immunoproteasomes compared to IFNγ treatment alone.

In summary, we provide evidence that the immunoproteasome is critically involved in the major aspects of innate immunity, including the complement system, phagocytosis and cytokine release. In addition, the data presented here suggest that immunoproteasomes modulate microglia immune response by regulating NF-κB activation. Finally, we show that NADH, a known proteasome interacting co-factor, can reduce levels of assembled immunoproteasomes in response to IFNγ and, by doing so, reduce the immune response.

Declarations

Acknowledgements

We thank Dr. Yumin Zhang for generously gifting the BV-2 cell lines, Dr. Joseph McCabe for fruitful discussions, Hikari Tanaka, Dr. Kelsey Voss and Dr. Michael Shaughness for technical assistance. These studies were supported by grants from the National Institute of Neurological Disorders and Stroke (R01NS091575) to BGB, Center for Neuroscience and Regenerative Medicine (CNRM), Grant number: CNRM-70-9238 to KEM and intramural startup funds from the Department of Defense to BGB.

Data availability

The data that support the findings of this study are available from the corresponding author upon reasonable request.

Author Contributions

K.E.M., S.I., G.K. and B.G.B. conceived the study, designed the experiments and wrote the paper; K.E.M., S.I., G.K., E.M.B., B.M.M., M.W.S., S.G.P, N.M.M., K.N.A. J.D.R. and B.G.B., conducted experiments, acquired and analyzed the data. All authors discussed the results and conclusions and reviewed the manuscript.

Competing Interests

Neither I nor my family members have a financial interest in any commercial product, service, or organization providing financial support for this research.

Disclaimer

The opinions and assertions expressed herein are those of the author(s) and do not reflect the official policy or position of the Uniformed Services University or the Department of Defense.

References

1. Kofler, J. & Wiley, C. A. Microglia: key innate immune cells of the brain. Toxicol Pathol 39, 103–114 (2011). https://doi.org/10.1177/0192623310387619
2. Veerhuis, R., Nielsen, H. M. & Tenner, A. J. Complement in the brain. Molecular immunology 48, 1592–1603 (2011). https://doi.org/10.1016/j.molimm.2011.04.003
3. Tanaka, S. *et al.* Activation of microglia induces symptoms of Parkinson's disease in wild-type, but not in IL-1 knockout mice. Journal of neuroinflammation 10, 143 (2013). https://doi.org/10.1186/1742-2094-10-143
4. Ciechanover, A. The ubiquitin-proteasome proteolytic pathway. Cell 79, 13–21 (1994).
5. Stohwasser, R. *et al.* Biochemical analysis of proteasomes from mouse microglia: induction of immunoproteasomes by interferon-gamma and lipopolysaccharide. Glia 29, 355–365 (2000).
6. Moritz, K. E. *et al.* The role of the immunoproteasome in interferon-gamma-mediated microglial activation. Scientific reports 7, 9365 (2017). https://doi.org/10.1038/s41598-017-09715-y
7. Ferrington, D. A. & Gregerson, D. S. Immunoproteasomes: structure, function, and antigen presentation. Progress in molecular biology and translational science 109, 75–112 (2012). https://doi.org/10.1016/B978-0-12-397863-9.00003-1
8. Dräger, N. M. *et al.* A CRISPRi/a platform in iPSC-derived microglia uncovers regulators of disease states. *bioRxiv*, 2021.2006.2016.448639 (2021). https://doi.org/10.1101/2021.06.16.448639
9. Fernandopulle, M. S. *et al.* Transcription Factor-Mediated Differentiation of Human iPSCs into Neurons. Curr Protoc Cell Biol 79, e51 (2018). https://doi.org/10.1002/cpcb.51
10. Bicker, H. *et al.* A simple assay to measure phagocytosis of live bacteria. Clinical chemistry 54, 911–915 (2008). https://doi.org/10.1373/clinchem.2007.101337
11. Singhrao, S. K., Neal, J. W., Morgan, B. P. & Gasque, P. Increased complement biosynthesis by microglia and complement activation on neurons in Huntington's disease. Experimental neurology 159, 362–376 (1999). https://doi.org/10.1006/exnr.1999.7170
12. Bojkowska, K. *et al.* Measuring in vivo protein half-life. Chemistry & biology 18, 805–815 (2011). https://doi.org/10.1016/j.chembiol.2011.03.014
13. Kouser, L. *et al.* Emerging and Novel Functions of Complement Protein C1q. Front Immunol 6, 317 (2015). https://doi.org/10.3389/fimmu.2015.00317
14. Maierhaba, M. *et al.* Association of the thyroglobulin gene polymorphism with autoimmune thyroid disease in Chinese population. Endocrine 33, 294–299 (2008). https://doi.org/10.1007/s12020-008-9082-x

15. Johnston, R. B., Jr., Klemperer, M. R., Alper, C. A. & Rosen, F. S. The enhancement of bacterial phagocytosis by serum. The role of complement components and two cofactors. The Journal of experimental medicine 129, 1275–1290 (1969).
16. Sacks, S., Zhou, W., Campbell, R. D. & Martin, J. C3 and C4 gene expression and interferon-gamma-mediated regulation in human glomerular mesangial cells. Clinical and experimental immunology 93, 411–417 (1993).
17. Becherer, J. D. & Lambris, J. D. Identification of the C3b receptor-binding domain in third component of complement. The Journal of biological chemistry 263, 14586–14591 (1988).
18. *European journal of immunology* 29, 1955–1965 (1999). https://doi.org/10.1002/(SICI)1521-4141(199906)29:06<1955::AID-IMMU1955>3.0.CO;2-O
19. Esparza, I., Fox, R. I. & Schreiber, R. D. Interferon-gamma-dependent modulation of C3b receptors (CR1) on human peripheral blood monocytes. Journal of immunology 136, 1360–1365 (1986).
20. Williams, K., Ulvestad, E. & Antel, J. P. B7/BB-1 antigen expression on adult human microglia studied in vitro and in situ. European journal of immunology 24, 3031–3037 (1994). https://doi.org/10.1002/eji.1830241217
21. Anthony, D. *et al.* CXC chemokines generate age-related increases in neutrophil-mediated brain inflammation and blood-brain barrier breakdown. Current biology: CB 8, 923–926 (1998).
22. Kossmann, T., Stahel, P. F., Morganti-Kossmann, M. C., Jones, J. L. & Barnum, S. R. Elevated levels of the complement components C3 and factor B in ventricular cerebrospinal fluid of patients with traumatic brain injury. Journal of neuroimmunology 73, 63–69 (1997).
23. Rappert, A. *et al.* CXCR3-dependent microglial recruitment is essential for dendrite loss after brain lesion. The Journal of neuroscience: the official journal of the Society for Neuroscience 24, 8500–8509 (2004). https://doi.org/10.1523/JNEUROSCI.2451-04.2004
24. Jiang, X. *et al.* Inhibition of LPS-induced retinal microglia activation by naloxone does not prevent photoreceptor death. Inflammation 36, 42–52 (2013). https://doi.org/10.1007/s10753-012-9518-6
25. Xanthou, G., Duchesnes, C. E., Williams, T. J. & Pease, J. E. CCR3 functional responses are regulated by both CXCR3 and its ligands CXCL9, CXCL10 and CXCL11. European journal of immunology 33, 2241–2250 (2003). https://doi.org/10.1002/eji.200323787
26. Thacker, M. A. *et al.* CCL2 is a key mediator of microglia activation in neuropathic pain states. European journal of pain 13, 263–272 (2009). https://doi.org/10.1016/j.ejpain.2008.04.017
27. Kang, Y. *et al.* Treg cell resistance to apoptosis in DNA vaccination for experimental autoimmune encephalomyelitis treatment. PloS one 7, e49994 (2012). https://doi.org/10.1371/journal.pone.0049994
28. Skuljec, J. *et al.* CCL5 induces a pro-inflammatory profile in microglia in vitro. Cellular immunology 270, 164–171 (2011). https://doi.org/10.1016/j.cellimm.2011.05.001
29. Louboutin, J. P. & Strayer, D. S. Relationship between the chemokine receptor CCR5 and microglia in neurological disorders: consequences of targeting CCR5 on neuroinflammation, neuronal death and regeneration in a model of epilepsy. CNS & neurological disorders drug targets 12, 815–829 (2013).

30. Bunting, K. *et al.* Genome-wide analysis of gene expression in T cells to identify targets of the NF-kappa B transcription factor c-Rel. Journal of immunology 178, 7097–7109 (2007).
31. Wickremasinghe, M. I., Thomas, L. H., O'Kane, C. M., Uddin, J. & Friedland, J. S. Transcriptional mechanisms regulating alveolar epithelial cell-specific CCL5 secretion in pulmonary tuberculosis. The Journal of biological chemistry 279, 27199–27210 (2004). https://doi.org/10.1074/jbc.M403107200
32. Suzuki, K. *et al.* Evidence that Escherichia coli ubiA product is a functional homolog of yeast COQ2, and the regulation of ubiA gene expression. Bioscience, biotechnology, and biochemistry 58, 1814–1819 (1994). https://doi.org/10.1271/bbb.58.1814
33. Ohmori, Y. & Hamilton, T. A. Cooperative interaction between interferon (IFN) stimulus response element and kappa B sequence motifs controls IFN gamma- and lipopolysaccharide-stimulated transcription from the murine IP-10 promoter. The Journal of biological chemistry 268, 6677–6688 (1993).
34. Adriouch, S. *et al.* NAD + released during inflammation participates in T cell homeostasis by inducing ART2-mediated death of naive T cells in vivo. Journal of immunology 179, 186–194 (2007).
35. Choi, H. A., Kim, M. R., Park, K. A. & Hong, J. Interaction of over-the-counter drugs with curcumin: influence on stability and bioactivities in intestinal cells. J Agric Food Chem 60, 10578–10584 (2012). https://doi.org/10.1021/jf303534e
36. Tsvetkov, P. *et al.* NADH binds and stabilizes the 26S proteasomes independent of ATP. The Journal of biological chemistry 289, 11272–11281 (2014). https://doi.org/10.1074/jbc.M113.537175
37. Fonseca, M. I. *et al.* Cell-specific deletion of C1qa identifies microglia as the dominant source of C1q in mouse brain. Journal of neuroinflammation 14, 48 (2017). https://doi.org/10.1186/s12974-017-0814-9
38. Heppner, F. L., Ransohoff, R. M. & Becher, B. Immune attack: the role of inflammation in Alzheimer disease. Nature reviews. Neuroscience 16, 358–372 (2015). https://doi.org/10.1038/nrn3880
39. Maphis, N. *et al.* Reactive microglia drive tau pathology and contribute to the spreading of pathological tau in the brain. Brain: a journal of neurology 138, 1738–1755 (2015). https://doi.org/10.1093/brain/awv081
40. Shi, Q. *et al.* Complement C3 deficiency protects against neurodegeneration in aged plaque-rich APP/PS1 mice. Sci Transl Med 9 (2017). https://doi.org/10.1126/scitranslmed.aaf6295
41. Bahrini, I., Song, J. H., Diez, D. & Hanayama, R. Neuronal exosomes facilitate synaptic pruning by up-regulating complement factors in microglia. Sci Rep 5, 7989 (2015). https://doi.org/10.1038/srep07989
42. Brown, G. C. & Neher, J. J. Microglial phagocytosis of live neurons. Nature reviews. Neuroscience 15, 209–216 (2014). https://doi.org/10.1038/nrn3710
43. Neher, J. J. *et al.* Phagocytosis executes delayed neuronal death after focal brain ischemia. Proceedings of the National Academy of Sciences of the United States of America 110, E4098-4107 (2013). https://doi.org/10.1073/pnas.1308679110

44. Neher, J. J., Neniskyte, U. & Brown, G. C. Primary phagocytosis of neurons by inflamed microglia: potential roles in neurodegeneration. Frontiers in pharmacology 3, 27 (2012). https://doi.org/10.3389/fphar.2012.00027
45. Neher, J. J. *et al.* Inhibition of microglial phagocytosis is sufficient to prevent inflammatory neuronal death. Journal of immunology 186, 4973–4983 (2011). https://doi.org/10.4049/jimmunol.1003600
46. Hong, S. *et al.* Complement and microglia mediate early synapse loss in Alzheimer mouse models. Science 352, 712–716 (2016). https://doi.org/10.1126/science.aad8373
47. Underly, R., Song, M. S., Dunbar, G. L. & Weaver, C. L. Expression of Alzheimer-Type Neurofibrillary Epitopes in Primary Rat Cortical Neurons Following Infection with Enterococcus faecalis. Front Aging Neurosci 7, 259 (2015). https://doi.org/10.3389/fnagi.2015.00259
48. Bitzer, A., Basler, M., Krappmann, D. & Groettrup, M. Immunoproteasome subunit deficiency has no influence on the canonical pathway of NF-kappaB activation. Molecular immunology 83, 147–153 (2017). https://doi.org/10.1016/j.molimm.2017.01.019
49. Jang, E. R. *et al.* Revisiting the role of the immunoproteasome in the activation of the canonical NF-kappaB pathway. Mol Biosyst 8, 2295–2302 (2012). https://doi.org/10.1039/c2mb25125f
50. Verdin, E. NAD(+) in aging, metabolism, and neurodegeneration. Science 350, 1208–1213 (2015). https://doi.org/10.1126/science.aac4854
51. Bose, S., Stratford, F. L., Broadfoot, K. I., Mason, G. G. & Rivett, A. J. Phosphorylation of 20S proteasome alpha subunit C8 (alpha7) stabilizes the 26S proteasome and plays a role in the regulation of proteasome complexes by gamma-interferon. The Biochemical journal 378, 177–184 (2004). https://doi.org/10.1042/BJ20031122

Figures

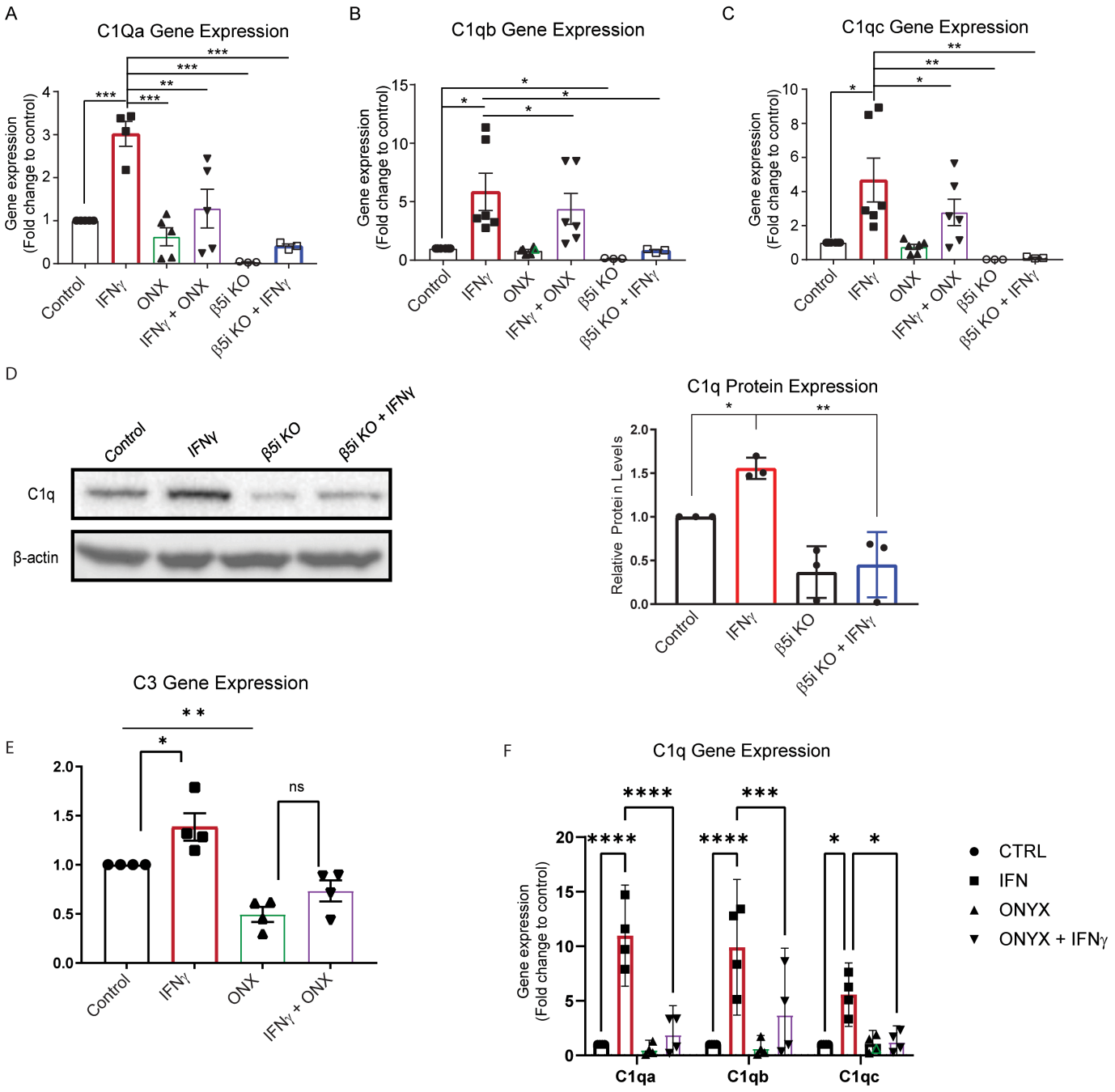

Figure 1

Immunoproteasome inhibition reduces IFNγ-dependent complement gene activation. Wild-type or β5i knockout BV-2 cells were treated with IFNγ in the absence and presence of immunoproteasome inhibitor, ONX-0914 and levels of C1q genes were analyzed. **A.** Gene expression analysis revealed a significant difference of C1qa gene expression between treatment groups ([F(5, 20) =9.21], $p<.001$, n=5). *Post hoc* analysis revealed that IFNγ resulted in a significant increase of C1qa compared to all other groups (control, $p<.001$; ONX-0914, $p=.001$; ONX+IFNγ, $p<.01$; KO control, $p<.001$; K.O. IFNγ, $p<.001$). C1qa levels

were not increased by IFNγ, in β5i KO cells (p=.996, n=3). **B.** Gene expression analysis revealed a significant difference of C1qb gene expression between treatment groups ([F(5, 20) =10.56], p<.001, n=5). *Post hoc* analysis revealed that IFNγ resulted in a significant increase of C1qb (control, p<.001; KO control, p<.001; KO IFNγ, p<.05. C1qb levels were not increased by IFNγ, in β5i KO cells (p=.974, n=3). **C.** Gene expression analysis revealed a significant difference of C1qc gene expression between treatment groups ([F(5, 24) =10.56], p<.001, n=6). *Post hoc* analysis revealed that IFNγ resulted in a significant increase of C1qc (control, p<.001; ONX+IFNγ, p=.012; KO control, p<.001; K.O. IFNγ, p<.01. C1qc levels were not increased by IFNγ, in β5i KO cells (p>.999, n=3). **D.** Western blot analysis confirms that IFNγ treatment increases C1q protein levels in WT BV2 cells but not in β5i KO BV-2 cells. **E.** Analysis of C3 gene expression revealed a significant difference between groups (F(3,12)=15.76, p<.001, n=4). *Post hoc* analysis revealed that ONX-0914 treatment reduced C3 levels compared to control and IFNγ treatments (p<.01 and $p \leq .001$, respectively). Further, ONX-0914 co-treatment with IFNγ reduced C3 levels compared to IFNγ alone, (p=.002). **F.** Gene expression analysis of C1qa, C1qb and C1qc in iPSC-derived microglia were determined by qRT-PRC (control n=4, SMA n=4; * p<0.05, ** p=0.01, *** p<0.001, **** P<.0001).

Izadjoo et al Figure 2

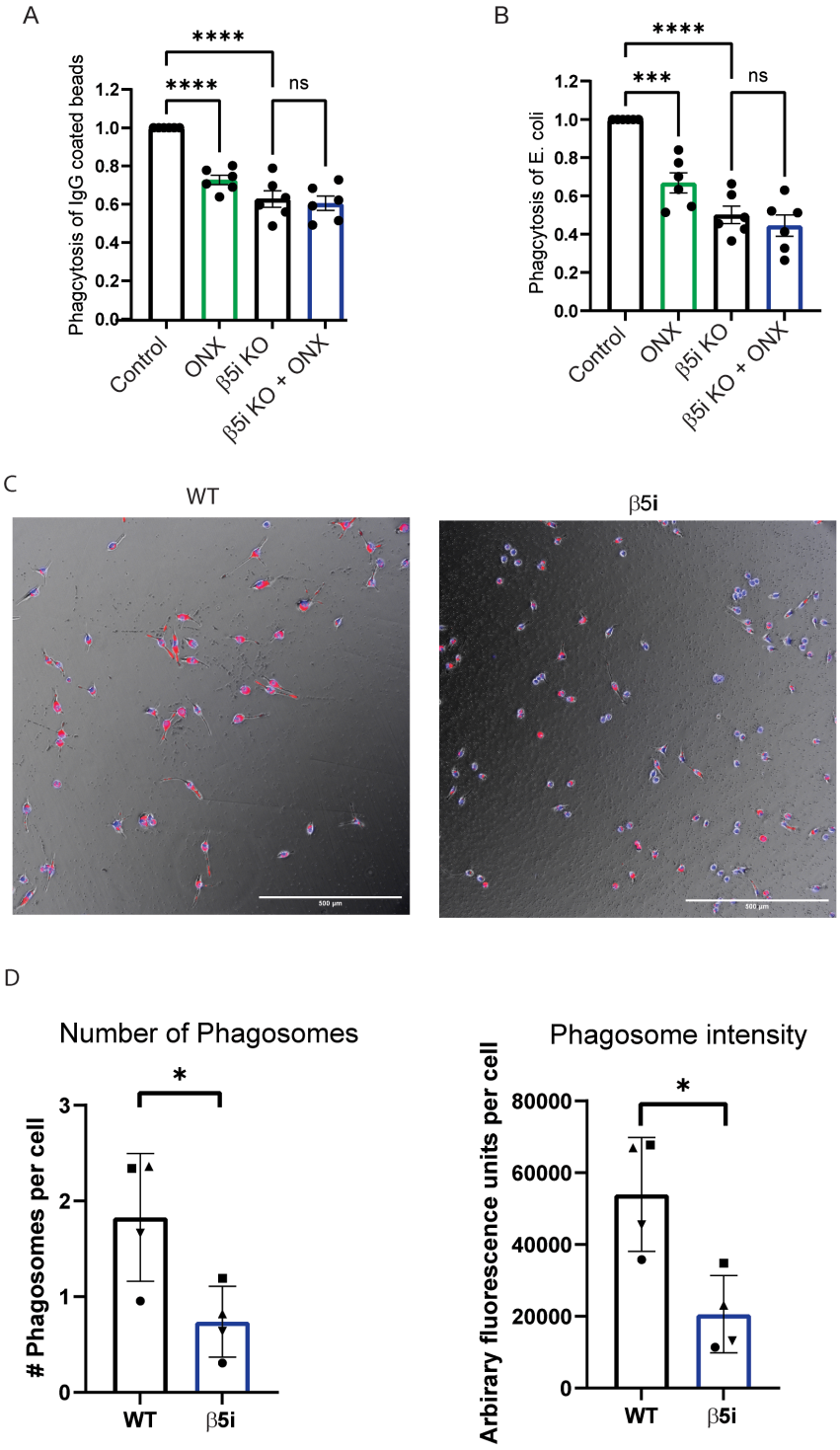

Figure 2

Phagocytosis is impaired by immunoproteasome inhibition. WT and β5i KO BV-2 cells were treated for 24 hours with ONX-0914 prior to measuring phagocytosis by flow cytometry. To adjust for background, control cells that were not exposed to fluorescent beads were used for each experiment **A.** Phagocytosis of IgG-coated latex beads was significantly different between groups ([F(3,10)=7.68, *p*=.005). *Post hoc* analysis revealed that treatment with ONX-0914 resulted in significantly decreased phagocytosis

compared to control (p=.032). **B.** Phagocytosis of eGFP-expressing E. coli was measured after a 30 minute incubation by quantifying the percentage of cells that were GFP positive. Flow cytometry analysis revealed a significant difference between treatment groups ([F(3,18)=39.23], p<.001). Treatment with ONX-0914 resulted in significantly decreased phagocytosis compared to control (p<.001). **C**. Example images of pHrodo IgG mediated phagocytosis uptake at end of 2-hour imaging in WT (left) and β5i KO BV-2 cells (right). Red fluorescence signifies pHrodo bead uptake. Blue fluorescence signifies Hoechst staining of cell nuclei. Scale bar is 500μm. **D**. Number of phagosomes per cell and mean phagosome signal intensity was significantly decreased in β5i KO BV-2 cells compared to WT. Reported as mean value per experiment. Error bars demonstrate SEM. Phagosome count per cell statistical analysis was performed with unpaired t-test, *p<0.0289. Mean phagosome fluorescence intensity analysis was performed with unpaired t-test, *p<0.0132.

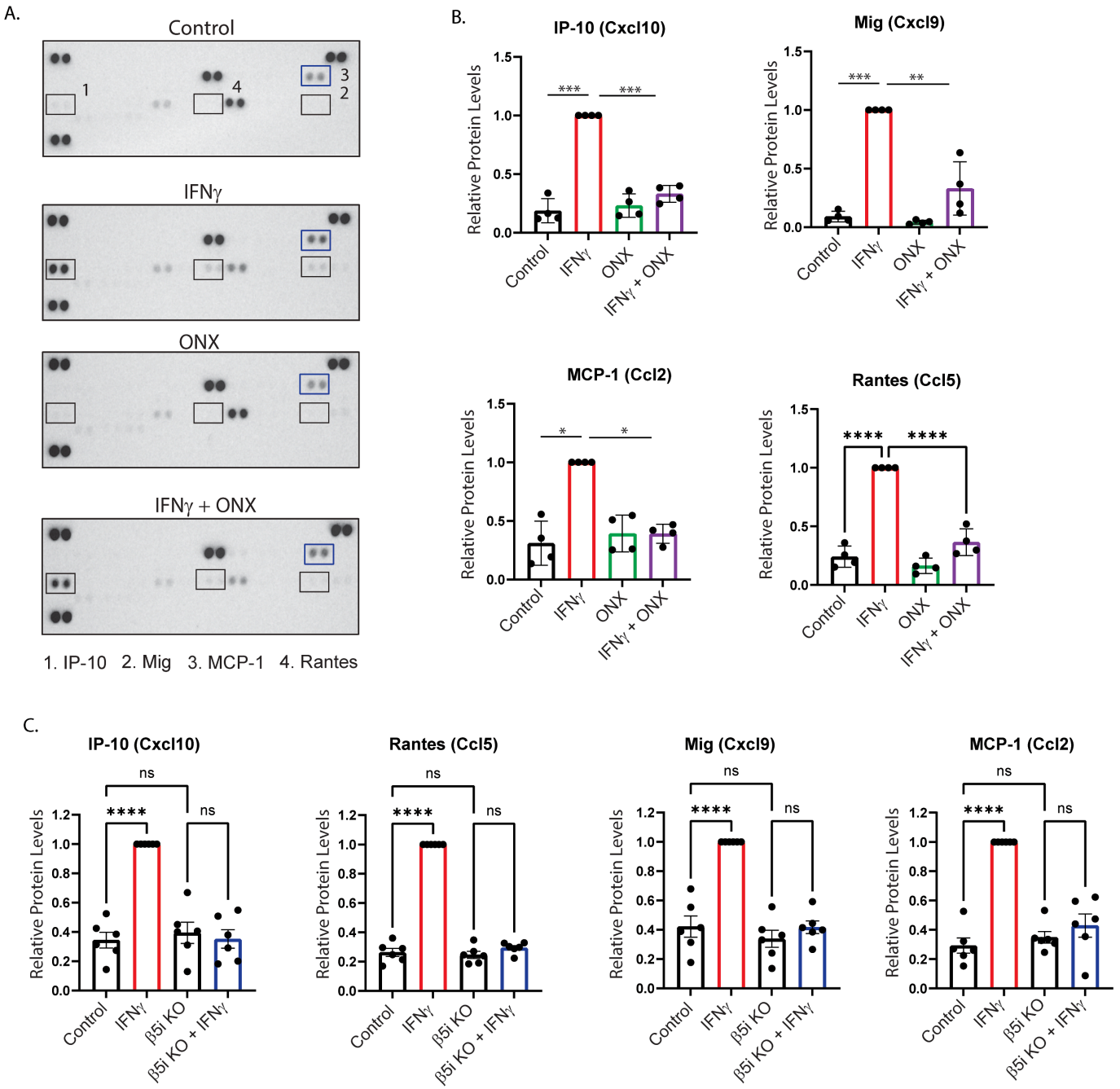

Figure 3

Immunoproteasomes mediate IFNγ-dependent cytokine production. BV-2 cells were treated for 24 hours, and cytokine levels were measured using a Proteome Profiler assay. **A and B.** Statistical analysis revealed that ONX-0914 treatment abrogated the IFNγ-dependent increase of Ip-10 ([F(3,11)=104.4], $p<.001$). *Post hoc* analysis revealed that IFNγ increased Ip-10 levels compared to control ($p<.001$), ONX-0914 ($p<.001$), and ONX-0914+IFNγ co-treatment ($p<.001$). In addition, there was a significant difference of Mig protein levels between treatment groups ([F(3,11)=18.61], $p<.001$). *Post hoc* analysis revealed that

IFNγ treatment resulted in higher Mig protein levels than all other groups (Ctrl,ontrol $p<.001$; ONX-0914, $p<.001$; ONX-0914+IFNγ, $p=.003$). MCP-1 levels were significantly different between groups ([$F(3,8)=5.591$], $p=.02$). IFNγ treatment increased MCP-1 levels compared to control ($p=.035$) which was reduced by ONX-0914 co-treatment ($p=.029$). Rantes protein levels were also different between treatment groups ([$F(3,12)=24.18$], $p<.001$). *Post hoc* analysis revealed that Rantes cytokine levels were significantly higher in the IFNγ treatment group compared to all other groups (Control, $p<.001$; ONX-0914, $p<.001$; ONX-0914, +IFNγ, $p<.0001$).. **C.** BV-2 β5i KO **c**ells were treated with IFNγ for 24 hours, and cytokine levels were measured using a Proteome Profiler assay. Ip-10, Mig, Rantes, and MCP-1 chemokine induction wasere abrogated in BV-2 β5i KO cells exposed to IFNγ, similar to ONX-0914 treatment.

Izadjoo et al Figure 4

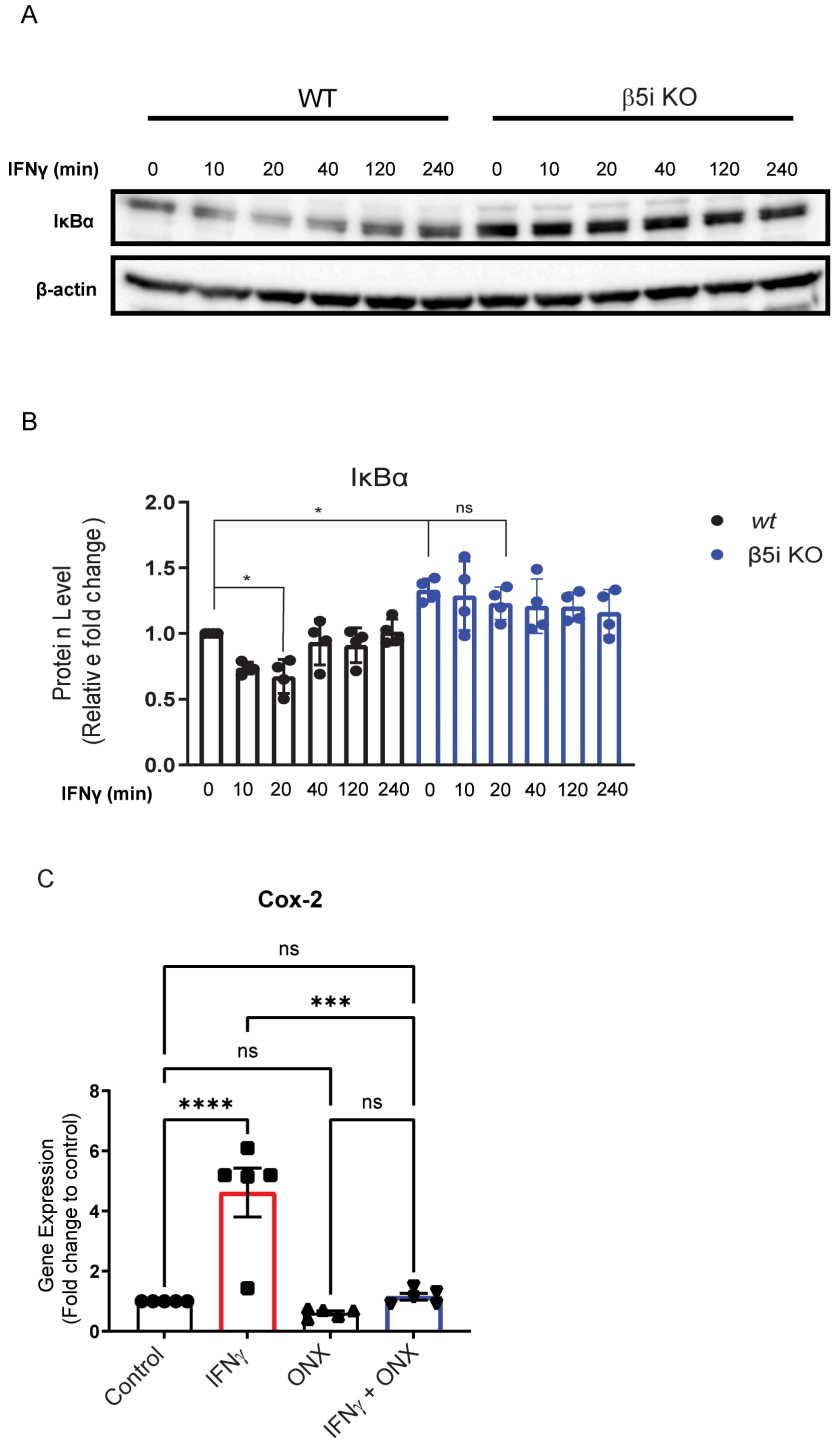

Figure 4

Altered degradation of IκBαin the absence of immunoproteasome activity. IκBα levels were measured in WT and β5i KO BV-2 cells in the absence and presence of IFNγ. **A.** Representative Western blot of IκBα in **WT** BV-2 and β5i KO BV-2 βcells over a 240 minute time course following IFNγ exposure. **B.** Quantification of the data represented in A. (n=4, *p<0.05, ns=no significance) . There was a significant difference between groups ([F(3,28)=12.75], *p*<.001). *Post hoc* analysis revealed that IFNγ treatment

significantly reduced IκBα levels compared to control (p<0.05) after 20 minutes. IκBα levels were unchanged in BV-2 β5i KO cells treated with IFNγ. **C**. Gene expression analysis of cox2C by qRT-PCR (n=5, ***p<0.001, ****p<0.0001, ns=no significance).

Izadjoo et al Figure 5

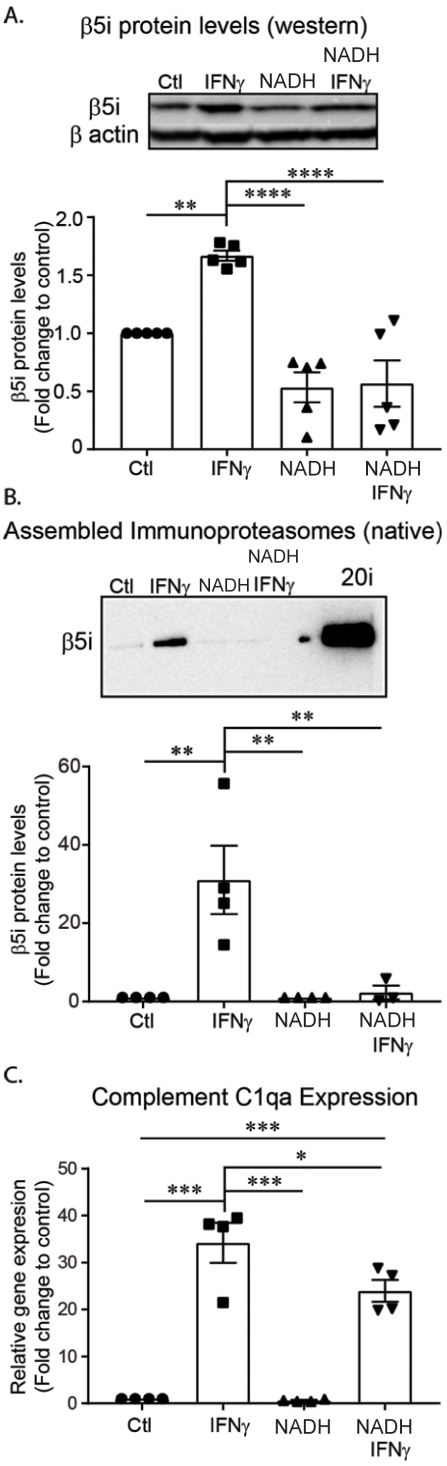

Figure 5

NADH blocks formation of the immunoproteasome. BV-2 cells were pre-treated with NADH for 24 hours, then treated with IFNγ for an additional 24 hours. Relative amounts of immunoproteasome protein levels

were quantified. **A.** Western blot analysis revealed a significant difference between treatment groups ([F(3, 16) =19.04], $p<.001$, n=4). *Post hoc* analysis revealed that IFNγ increasesd total β5i protein levels compared to all groups (Control, $p=.006$; NAD, $p<.001$; NADH+IFNγ, $p<.0001$). Further, IFNγ did not significantly increase β5i protein levels in cells pre-treated with NADH ($p=.997$). **B.** Assembled immunoproteasomes (20i represents purified positive control) were measured using native gel electrophoresis. Analysis revealed that there was a significant difference between treatment groups ([F(3, 11) =9.845], $p=.002$, n=4). *Post hoc* analysis revealed that IFNγ increased the amount of assembled immunoproteasomes compared to all treatment groups (Control, $p=.003$; NADH, $p=.004$; NAD+IFNγ, $p=.009$). Interestingly, when cells are pre-treated with NADH, immunoproteasomes are not increased in response to IFNγ ($p=.996$). C. To determine if NADH treatment would successfully reduce complement activation in BV-2 cells, we pre-treated with NADH, then measured gene expression of complement activator C1qa. An ANOVA revealed a significant treatment effect ([F(3,12)=48.22, $p<.001$). *Post hoc* analysis revealed a significant increase of C1qa gene expression in response to IFNγ treatment ($p<.001$), an effect that was reduced by NADH pre-treatment ($p=.049$).

Supplementary Files

This is a list of supplementary files associated with this preprint. Click to download.

- SupplemantalFigureLegends.docx
- SupplementalFigures01.tif
- SupplementalFigures02.tif
- SupplementalFigures03.tif